Mater. Res. Soc. Symp. Proc. Vol. 892 © 2006 Materials Research Society 0892-FF06-05.1

Carrier Recombination, Relaxation, and Transport Dynamics in InN

Fei Chen and Alexander N. Cartwright
Department of Electrical Engineering, University at Buffalo,
State University of New York, Buffalo, New York 14260
Hai Lu and William J. Schaff
Department of Electrical and Computer Engineering, Cornell University,
Ithaca, New York 14853

ABSTRACT

Knowledge of the carrier recombination, relaxation, and transport processes in InN materials is essential for determining the applicability of this material system in photonic and electronic applications. In this article, we provide a review of time-resolved spectroscopy experimental techniques and our recent results using these techniques to measure transient processes in InN. Specifically, subpicosecond differential transmission experiments were used to determine the carrier recombination lifetime and the carrier thermalization time of InN. In those experiments, we observed a fast initial hot carrier cooling followed by a slower recombination process. At short times after pulsed excitation, modeling of the observed relaxation suggests that the dominant energy relaxation process is longitudinal optical phonon scattering modified by a strong hot phonon effect at room temperature. An inverse proportionality between the carrier lifetime and the free electron concentration was found. This suggests that donor-like defects or impurities may stimulate the formation of non-radiative recombination centers. Furthermore, we report the measurements of in-plane carrier transport and hole mobility of an InN epilayer by time-resolved transient grating spectroscopy using subpicosecond pulses at 800 nm and ~1900 nm for grating writing and probing, respectively. The ambipolar diffusion coefficient $D_a = 2.0$ cm^2/s and hole mobility $\mu_h = 39$ cm^2/Vs at 300 K near the InN surface were determined by monitoring the transient grating kinetics at various grating periods.

INTRODUCTION

During the past three years, InN has attracted significant research interest primarily because of an intense debate over its bandgap. Moreover, this interest has intensified because of the promise of devices that can be enabled by the observation of high electron mobility and saturation velocity [1, 2] and small bandgap [3-6] in InN epilayers. These properties make these materials promising for high electron mobility transistors, high-efficiency solar cells, and infrared emitters and photodetectors. Recent advances in the synthesis of single crystalline InN indicate that the quality of InN is rapidly approaching the level required for application in practical devices [7-10]. Notwithstanding these important demonstrations, low bandgap InN is still a relatively new III-Nitride material with many of it's properties still not adequately measured.

In spite of all the recent progress on the measurement and calculation of the physical and optical properties of InN, there has been relatively few papers on time-resolved spectroscopy of InN [11-15]. Linear optical spectroscopy of InN has provided invaluable information on many diverse aspects, such as the bandgap energy, electronic band structure, phonons, defects, etc. Optical excitation has the ability to generate a non-equilibrium carrier distribution, and optical

spectroscopy provides an excellent means of determining such distribution functions. A powerful tool for investigating a wide diversity of ultrafast carrier phenomena, such as carrier recombination, relaxation, diffusion, and transport dynamics, in semiconductors and semiconductor nanostructures is enabled when optical spectroscopy is combined with ultrafast laser pulses. Typically, these mechanisms are not easily assessed through other techniques. For example, the Hall method can be used to determine the electron mobility in InN [16]. However, the presence of a high unintentional *n*-type doping level in InN, that compensates any p-type doping, hampers the use of the Hall method for measuring the hole mobility and the hole diffusion length. In contrast, the time-resolved transient grating technique has the unique strength and flexibility to temporally resolve the photoexcited carrier relaxation, recombination, and diffusion in InN with subpicosecond resolution.

Recently, we have performed time-resolved spectroscopy measurements of carrier recombination lifetimes, carrier thermalization time, and hole mobility of InN epilayers [17-21]. These parameters are essential to the design and optimization of optoelectronic devices and high-speed electronic devices based on such materials as well as in optimizing material growth conditions. It is important to realize that, to date, there is insufficient information to determine the future applications of low bandgap InN materials for visible to IR optical devices. However, it is our belief that improvements in materials quality will progress parallel with improvements in the knowledge of the fundamental properties of these materials. Therefore, in this article we will review the experimental techniques and our most important results regarding the time-resolved optical spectroscopy of InN, as well as the future directions.

EXPERIMENTAL TECHNIQUES

Two time-resolved optical spectroscopy techniques will be discussed in detail in this paper. The first technique is the time-resolved differential transmission technique that provides a direct measurement of carrier recombination and relaxation dynamics. The second technique is the time-resolved transient grating technique that is devoted to measuring the carrier diffusivity and in-plane carrier transport of InN. This technique is based on the formation of a photogenerated carrier modulation (grating) by two interfering pulsed laser beams, and the detection of the diffraction of a third probe beam off this grating. The decay of the diffraction efficiency allows one to monitor the carrier diffusion dynamics. In this method, the simultaneous determination of ambipolar diffusion coefficient, hole mobility, and carrier lifetime in InN is possible.

(i) Time-resolved Differential Transmission

The schematic setup used for time-resolved differential transmission is shown in Fig. 1. Briefly, the output of a regenerative amplifier (REGA) is frequency doubled to 400 nm to serve as the pump source for a visible optical parametric amplifier (OPA) that generates a tunable infrared idler pulse (0.9 μm to 3.6 μm) with typical pulse widths of ~200 fs. The infrared pulse, which is tuned to a wavelength near the band edge of InN, is sent to a computer controlled delay stage and then tightly focused onto the sample. The transmitted probe beam is collected and focused to the InGaAs detector. In these experiments, the remaining output of REGA at 800 nm is used as the pump beam. A mechanical chopper is used to modulate the pump beam at a frequency of f_1, and modulate the probe beam at a frequency of f_2. The differential transmission signal is detected by standard lock-in techniques at the sum frequency of $f_1 + f_2$ to measure the

difference in the probe transmission (ΔT) with and without the pump present as a function of probe wavelength.

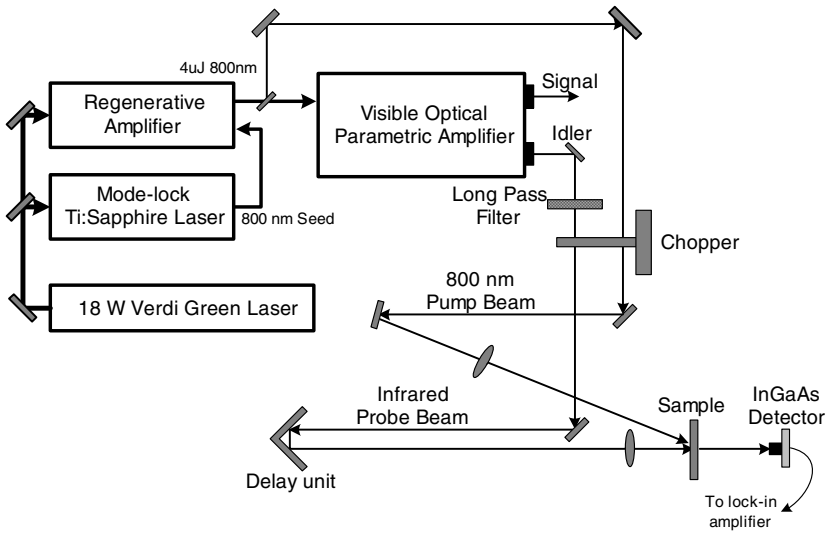

Figure 1. Schematic setup of a typical time-resolved differential transmission measurement of InN.

In differential transmission measurements, $\Delta T/T$ is directly proportional to the change of the interband absorption coefficient, $\Delta\alpha$, and is given by $\Delta T/T = e^{-\Delta\alpha d} - 1 \approx -\Delta\alpha d$, where d is the length of the active region. The photogenerated carriers excited by the pump pulse leads to a filling of electron and hole states in the corresponding bands. This band filling reduces the absorption of the probe beam and increases the probe transmission through the sample. The effect of the band filling on the absorption coefficients corresponds to the distribution of photogenerated carriers, and is described by [22, 23]: $\Delta\alpha(\lambda) = -\alpha_0(\lambda)\times\left[f_e(\lambda) + f_h(\lambda)\right]$, where f_e and f_h are the quasi-Fermi functions for electrons and holes, respectively. As a result, the measurements of temporal dependence of the change in transmission $\Delta T/T$ at different energy levels allow us to monitor the carrier distribution as well as the carrier recombination and relaxation dynamics.

(ii) Time-resolved Transient Grating

Transient grating experiments are performed by using ultrafast laser pulses at an energy above the bandgap and at an energy near the bandgap of InN for grating writing and probing, respectively. Specifically, the tunable infrared pulse (0.9 μm to 3.6 μm) with typical pulse widths of ~100 fs generated from the idler output of the visible OPA serves as the grating probe. Two coherent pump laser pulses are focused onto the same spot on the sample for the grating writing. The direct absorption of the two interfering pump pulses creates a thin free carrier grating with fringe spacing of $\Lambda = \lambda_{pump}/[2\sin(\theta/2)]$, where θ is the angle between the two incident beams, as shown in Fig. 2. After pulsed excitation, the grating decays by both in-plane ambipolar diffusion and carrier recombination. A time-delayed infrared probe pulse from the OPA is focused onto the optically excited region of the sample. The diffracted probe beam is then detected by an InGaAs detector. This technique allows us to monitor electron-hole distribution, $N(x)$, as a function of time via the time-varying diffraction efficiency of the grating.

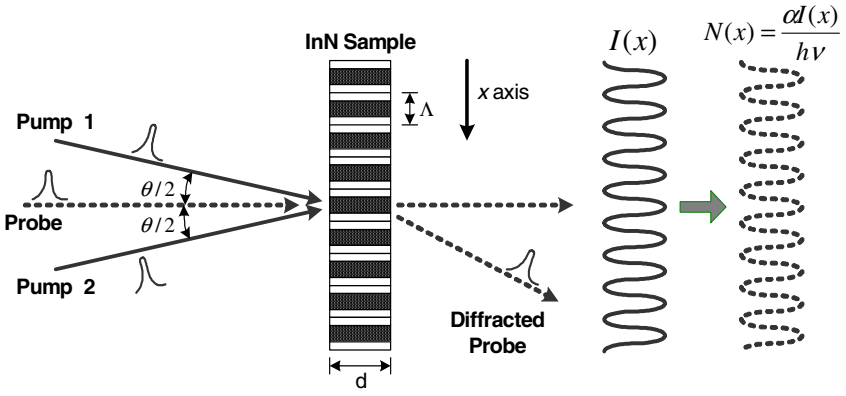

Figure 2. Two temporally and spatially pump beams create a carrier concentration induced grating for time-resolved transient grating measurements. A time-delayed probe pulse diffracts off of the grating and provides information on grating decay. $I(x)$ represents the optical intensity modulation generated by the interference of two pump beams and $N(x)$ is the corresponding photogenerated carrier distribution.

Due to the carrier induced changes in the absorption and refractive index, this carrier distribution forms a mixed amplitude-phase grating from which the probe can be diffracted. When assuming a monomolecular recombination, the decay rate τ_G is given by [24, 25]

$$\frac{1}{\tau_G} = \frac{1}{\tau_R} + \frac{4\pi^2 D_a}{\Lambda^2} \qquad (1)$$

where τ_R is the carrier recombination lifetime, D_a is the ambipolar diffusion coefficient, and Λ is the grating period. The grating period can be adjusted by varying the angle θ between two pump beams. Thus, Eq. (1) indicates that the slope and the crossing point to the axis of ordinate in a $1/\tau_G$ vs $4\pi^2/\Lambda^2$ plot directly provides the ambipolar diffusion coefficient and the reciprocal of the carrier lifetime, respectively.

RESULTS AND DISCUSSION

As mentioned earlier, we have developed the aforementioned ultrafast spectroscopic tools for the characterization of carrier dynamics of InN [17-21]. Specifically, we have successfully employed the time-resolved differential transmission (transmission type pump/probe) technique as a direct method for monitoring carrier recombination and relaxation in InN with femtosecond resolution, and determined the carrier lifetime and carrier thermalization time in such material. The most important results we have achieved regarding the recombination and relaxation dynamics of InN will be addressed in the following.

Fig. 3(a) shows the measured differential transmission signal as a function of time delay at various probed photon energies for a typical InN epilayer. The sample was a single crystalline 850 nm InN film grown on a 220 nm GaN buffer layer that was deposited on a (0001) sapphire substrate by molecular beam epitaxy (MBE). The free electron concentration in this sample was measured to be 1.3×10^{18} cm^{-3} and the electron mobility was measured as 1340 cm^2/V·s at room temperature. The signal at the energy below 0.67 eV decays exponentially with time delay. In contrast, for energies above 0.67 eV, the signal shows an initial fast decay followed by a much slower relaxation. The fast decay component results from the relaxation of photoexcited hot

carriers. The slow decay component is attributed to the carrier recombination process. Recombination lifetimes ranging from 300 ps to 400 ps can be extracted by the exponential fit. Moreover, the signal at very short time delay immediately after pulse excitation as shown in Fig. 3(a) clearly indicates a hot carrier relaxation process in InN, which is reflected by an observed fast decay at an energy of 0.87 eV and a slight increase at an energy of 0.67 eV.

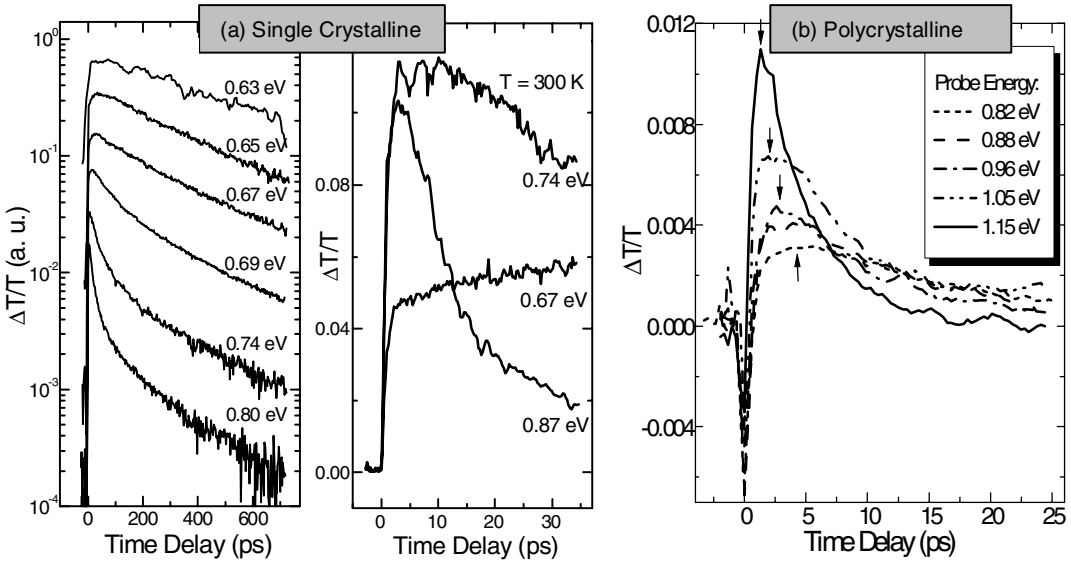

Figure 3. Differential transmission signal of (a) a single crystalline InN epilayer and (b) a polycrystalline InN sample as a function of time at different probe energies. The arrows in Fig.3 (b) indicate the maximum position at each differential transmission signal.

Similar measurements have also been performed on a polycrystalline sample, as shown in Fig. 3(b). In this case, the sample was grown on a silica glass substrate by plasma assisted MBE with an RF inductively coupled nitrogen source. The free electron concentration was measured as ~10^{20} cm^{-3}. In contrast to the measurements for the single crystalline sample, we observed a much faster carrier recombination rate for the polycrystalline sample, with a typical decay time of ~10 ps. Consistent with our understanding of hot carrier relaxation process after pulsed excitation, at higher probe energy the signal shows a faster decay, while the signal shows an initial rise followed by a slow decay for a low energy probe. Interestingly, we observed a sharp negative peak around zero time delay, where the width corresponds to the laser pulse width ~200 fs. The possible explanations could be two photon absorption or other coherent effects.

Fig. 4 shows the differential transmission spectra of the single crystalline sample for the time delay from 6 ps to 40 ps. At the earliest time the spectrum is very broad and the high-energy tail is exponentially decaying with energy. With increasing time delay, the spectra becomes narrower indicating the relaxation of the hot photoexcited carriers, and the exponential tails become steeper indicating a decrease in the carrier temperature. For energies sufficiently higher than the quasi-Fermi energy, one would expect the spectrum to decay exponentially, reflecting the Maxwell-Boltzman distribution of electrons and holes. We have deduced the carrier temperature from the spectra at various time delays by fitting the high-energy tails and plotted the carrier temperatures versus the time delay in the inset graph of Fig. 4. We observed that it takes approximately 10 ps for the carrier temperature to reach the lattice temperature. An energy relaxation model has been used to fit the results, and it suggests that the hot carrier cooling

process of InN at room temperature is dominated by the LO phonon scattering which is modified by a strong hot phonon screening effects [18].

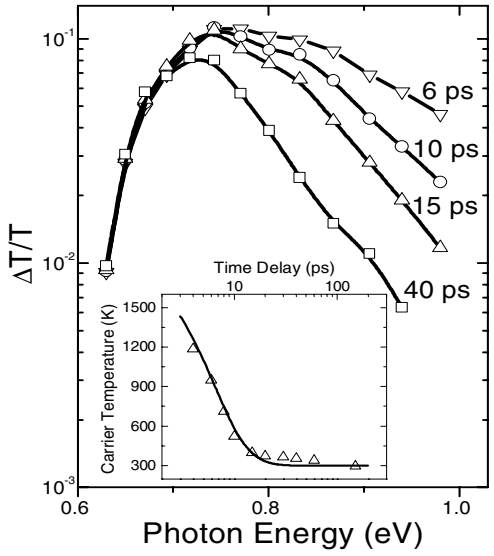

Figure 4. Differential transmission spectra at very short time delays. The inset graph shows the deduced carrier temperature vs. time delay [18].

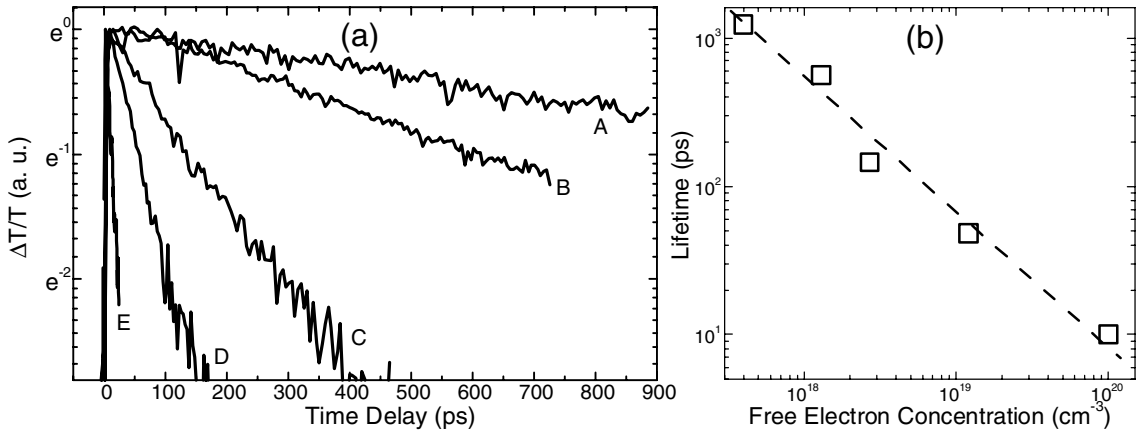

Figure 5. (a) Differential transmission signal as a function of time delay for InN epilayers with different crystalline quality. (b) Carrier lifetime as a function of free electron concentration.

Fig. 5 (a) shows the measured carrier recombination lifetime for several InN samples with different crystalline quality at room temperature. The unintentionally doped InN films were grown on (0001) sapphire with different buffer layers by molecular beam epitaxy. The structures contain (i) sample A, GaN(300 nm)/$In_{0.65}Ga_{0.35}N$(110 nm)/InN(7500 nm); (ii) sample B, GaN(220 nm)/InN(850 nm); (iii) sample C, AlN(300 nm)/InN(350 nm); and (iv) sample D, GaN(220 nm)/InN(600 nm). Sample E was a polycrystalline sample which has been previously addressed. Carrier lifetimes ranging from 10 ps to 1.3 ns have been extracted by a single exponential fit of the differential transmission signal in these samples. An inverse proportionality

between the carrier lifetime and the free electron concentration was observed as shown in the Fig. 5 (b) and suggests that the donor-like defects or impurities may stimulate a formation of non-radiative recombination centers, reducing the carrier lifetime [19].

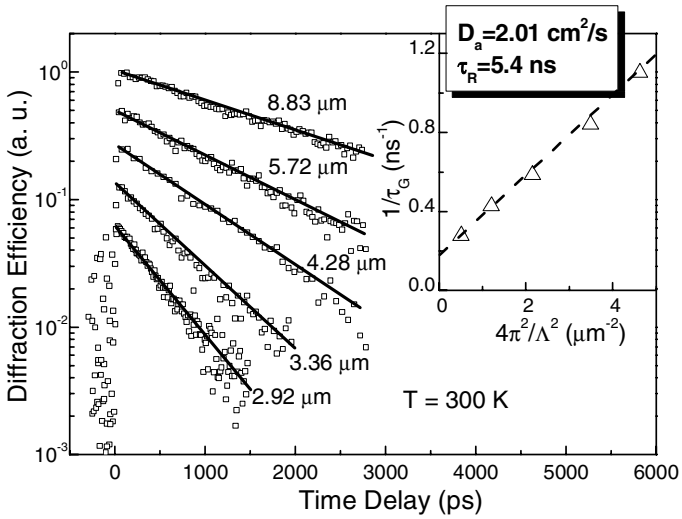

Figure 6. The grating diffraction efficiency as a function of the probe delay time at the front side of an InN epilayer for different grating periods. Solid lines indicate the single exponential fit. The inset graph shows the inverse grating decay time $1/\tau_G$ as a function of $4\pi^2/\Lambda^2$.

Time-resolved transient grating techniques have also been performed for the measurements of carrier diffusion and in-plane carrier transport dynamics of InN. Fig. 6 shows the decay of the grating diffraction efficiency as a function of time delay for a set of different grating periods, at the front side of an InN epilayer sample. The epilayer studied here was a 5.5 μm InN film grown on a 200 nm GaN buffer layer that was deposited on a (0001) sapphire substrate by molecular beam epitaxy. The electron Hall mobility and free electron concentration at room temperature were measured by Hall method as 2100 cm^2/Vs and 3.7×10^{17} cm^{-3} respectively. The diffraction efficiency as a function of time in each case exhibits a single exponential decay. More importantly, as shown in the inset graph of Fig. 6, the plot of decay time, $1/\tau_G$, vs $4\pi^2/\Lambda^2$ is a straight line, where the slope determines the ambipolar diffusion coefficient and the intercept gives the reciprocal of the carrier lifetime according to Eq. (1). Thus, the ambipolar diffusion coefficient of 2.01 cm^2/s and the carrier lifetime of 5.4 ns are extracted, respectively, for the measured sample.

Physically, the significant difference between the effective electron and hole masses and mobilities results in ambipolar diffusivity. An electric field will develop due to the faster moving electrons with respect to the more slowly moving holes. This field will result in a coupling of the motion of the electrons and holes and results in a coupled diffusive motion. In the case of equal electron and hole densities, the ambiploar diffusion coefficient is determined in terms of the mobilities by:

$$D_a = \frac{k_B T}{q}\left(\frac{2\mu_e\mu_h}{\mu_e+\mu_h}\right) \qquad (2)$$

where k_B is Boltzmann constant, q is the magnitude of the electronic charge, T is the carrier temperature, and μ_e and μ_h represent the electron and hole mobilities. Due to a much heavier

effective hole mass in InN, the electron mobility is assumed to be significantly larger than the hole mobility and thus Eq. (2) can be simplified as: $D_a \approx 2k_B T\mu_h / q$, which enables us to directly estimate the hole mobility. Accordingly, the estimated hole mobility and the corresponding hole diffusion length, $L_h = \sqrt{\frac{k_B T}{q}\mu_h \tau_R}$, of the InN epilayer, was deduced as 39 cm^2/Vs and 0.74 μm near free surface.

CONCLUSIONS AND FUTURE DIRECTIONS

In summary, we have reviewed our recent time-resolved spectroscopy measurements of InN. Subpicosecond time-resolved differential transmission and transient grating techniques have been utilized to investigate the carrier recombination, relaxation, diffusion, and transport processes of InN epilayers. Our results have provide direct measurements of carrier recombination lifetime, carrier thermalization lifetime, ambipolar diffusion coefficient, and hole mobility, which are not easily accessed by other techniques.

In spite of the research progress regarding the time-resolved spectroscopy of InN, much more work still needs to be done to completely characterize this material. Detailed knowledge of carrier lifetimes and transport mechanisms are needed for material improvement and for subsequent device development and modeling. For instance, it is possible to optically monitor the carrier recombination and transport dynamics near the surface/interface of InN and to directly determine the surface/interface recombination velocities by using the time-resolved differential transmission technique with tunable wavelength excitation in conjunction with the time-resolved transient grating technique. Quantum well structures with an InN thin film as the active layer will be the template for infrared emitters based on such materials. The carrier capture, carrier tunneling, carrier relaxation and recombination dynamics in the InN quantum well samples can be easily resolved through the two-color time-resolved differential transmission measurements. In addition, it is of great interest to employ polarization-resolved subpicosecond pump/probe differential transmission spectroscopy for the investigation of spin dynamics and for the determination of the electron spin relaxation time of InN. InN based devices may well play a critical role in the future of spintronics.

ACKNOWLEDGEMENTS

This work was partially supported by the National Science Foundation CAREER Award, NSF No. 9733720, and the Office of Naval Research Young Investigator Program Award No. N00014-00-1-0508 under the direction of Dr. Colin Wood. The work at Cornell University was supported by ONR under contract No. N000149910936.

REFERENCES

1. E. Bellotti, B. K. Doshi, K. F. Brennan, J. D. Albrecht, P. P. Ruden, *Journal of Applied Physics* **85**, 916 (1999).
2. S. K. O'Leary, B. E. Foutz, M. S. Shur, U. V. Bhapkar, L. F. Eastman, *Journal of Applied Physics* **83**, 826 (1998).

3. A. G. Bhuiyan, K. Sugita, K. Kasashima, A. Hashimoto, A. Yamamoto, V. Y. Davydov, *Applied Physics Letters* **83**, 4788 (2003).
4. V. Y. Davydov, A. A. Klochikhin, R. P. Seisyan, V. V. Emtsev, S. V. Ivanov, F. Bechstedt, J. Furthmuller, H. Harima, V. Mudryi, J. Aderhold, O. Semchinova, J. Graul, *Physica Status Solidi B-Basic Research* **229**, R1 (2002).
5. T. Inushima, V. V. Mamutin, V. A. Vekshin, S. V. Ivanov, T. Sakon, M. Motokawa, S. Ohoya, *Journal of Crystal Growth* **227**, 481 (2001).
6. J. Wu, W. Walukiewicz, K. M. Yu, J. W. Ager, E. E. Haller, H. Lu, W. J. Schaff, Y. Saito, Y. Nanishi, *Applied Physics Letters* **80**, 3967 (2002).
7. E. Kurimoto, H. Harima, A. Hashimoto, A. Yamamoto, *Physica Status Solidi B-Basic Research* **228**, 1 (2001).
8. A. Yamamoto, T. Tanaka, K. Koide, A. Hashimoto, *Physica Status Solidi a-Applied Research* **194**, 510 (2002).
9. H. Lu, W. J. Schaff, J. Hwang, H. Wu, W. Yeo, A. Pharkya, L. F. Eastman, *Applied Physics Letters* **77**, 2548 (2000).
10. H. Lu, W. J. Schaff, L. F. Eastman, J. Wu, W. Walukiewicz, V. Cimalla, O. Ambacher, *Applied Physics Letters* **83**, 1136 (2003).
11. Y. M. Chang, C. T. Chuang, C. T. Chia, K. T. Tsen, H. Lu, W. J. Schaff, *Applied Physics Letters* **85**, 5224 (2004).
12. R. Intartaglia, B. Maleyre, S. Ruffenach, O. Briot, T. Taliercio, B. Gil, *Applied Physics Letters* **86**, 142104 (2005).
13. W. Liang, K. T. Tsen, D. K. Ferry, H. Lu, W. J. Schaff, *Applied Physics Letters* **84**, 3849 (2004).
14. W. Liang, K. T. Tsen, D. K. Ferry, H. Lu, W. J. Schaff, *Applied Physics Letters* **84**, 3681 (2004).
15. K. T. Tsen, C. Poweleit, D. K. Ferry, H. Lu, W. J. Schaff, *Applied Physics Letters* **86**, 222103 (2005).
16. C. H. Swartz, R. P. Tompkins, N. C. Giles, T. H. Myers, H. Lu, W. J. Schaff, L. F. Eastman, *Journal of Crystal Growth* **269**, 29 (2004).
17. F. Chen, Cartwright A. N, Hai Lu, and W. J. Schaff, *Applied Physics Letters* **87**, 212104 (2005).
18. F. Chen, A. N. Cartwright, H. Lu, W. J. Schaff, *Applied Physics Letters* **83**, 4984 (2003).
19. F. Chen, A. N. Cartwright, H. Lu, W. J. Schaff, *Journal of Crystal Growth* **269**, 10 (2004).
20. F. Chen, A. N. Cartwright, H. Lu, W. J. Schaff, *Physica E-Low-Dimensional Systems & Nanostructures* **20**, 308 (2004).
21. F. Chen, A. N. Cartwright, H. Lu, W. J. Schaff, *Physica Status Solidi A-Applications and Materials Science* **202**, 768 (2005).
22. E. Wintner, *Journal of Applied Physics* **57**, 1533 (1985).
23. J. Shah, R. F. Leheny, C. Lin, *Solid State Communications* **18**, 1035 (1976).
24. D. S. Mccallum, A. N. Cartwright, X. R. Huang, T. F. Boggess, A. L. Smirl, T. C. Hasenberg, *Journal of Applied Physics* **73**, 3860 (1993).
25. X. R. Huang, D. S. Mccallum, M. D. Dawson, A. L. Smirl, T. F. Boggess, T. C. Hasenberg, R. L. Tober, *Journal of Applied Physics* **74**, 1868 (1993).